13. Martian Cratering and Implications for the Chronostratigraphy

The record of large impact basins on different planetary bodies allows us to compare the characteristics of the heavy bombardment period and the end of planetary formation. Both the cratering record itself and the age distribution of the impact basins represent the period of highest impactor flux, decaying rapidly within the first half billion years of our solar system. In order to test the plausibility of the Martian chronology model (see Chapter 5), the ages of the large Martian impact basins, using the derived Martian production function, were determined and compared to lunar basin ages. For the Moon, the large basins were produced no later than about 3.8 to 3.9 Ga ago and a similar situation should exist for Mars, following the marker horizon idea (Wetherill, 1975). This idea is based on the assumption that solar system bodies have undergone a similar evolution since planetary formation. In the cratering record on any solid surface body, which has representative large old surface units, this first period of heavy bombardment is present in the general crater size–frequency distribution as well as the large basin record itself. According to our investigation, the oldest surface areas on Mars, roughly the Martian southern highlands, e. g. Noachis Terra, were formed between 4.0 to 4.2 Ga ago during the period of heavy bombardment (Fig. 13.1). On the basis of crater counts of unambiguously defined craters, older surface units have not been found.

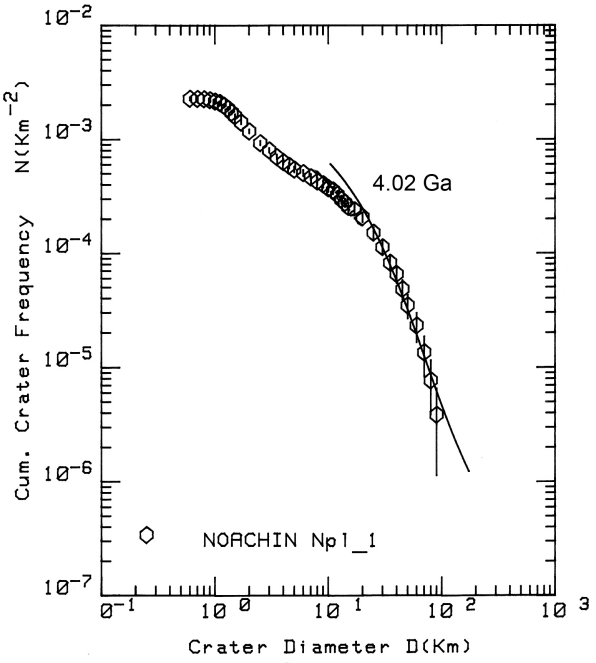

Figure 13.1.: The crater size frequency distribution measured for one of the oldest regions on Mars: Noachis Terra (map nomenclature: unit Npl1).

There have been attempts by Frey *et al.* (2002) to count so–called quasi–circular depressions, many of which are clearly seen in the Mars Orbiter Laser Altimeter (MOLA) elevation data, but generally not visible in available imagery. These depressions are interpreted as remnants of strongly eroded (highlands) or deeply buried (lowlands) craters produced early in Martian history. These measurements indicate that the buried lowland surface is older than the visible highland surface, where crater count ages are based on craters clearly recognized by their morphology.

During the Mars Global Surveyor Mission, vector magnetic field observations of the Martian crust were acquired. The location of observed magnetic field sources of multiple scales, strength, and geometry correlates remarkably well with the ancient cratered terrain of the Martian highlands (Acuña *et al.*, 1999). On the other hand, these (magnetic field) sources are absent in the lowland plains, near large impact basins such as Hellas and Argyre, and in most of the volcanic regions. Formation ages of these features will give a time–frame for the thermodynamical evolution of Mars as will be discussed in Part IV.

13.1. Martian Impact Basin Ages

Large Martian impact basins are randomly distributed in the heavily cratered highlands. The interior of any basin cannot be considered as pristine and crater counts would not indicate the formation age. In this study, we tried to identify units that best represent the formation age for a particular basin. Therefore, we chose a relatively narrow band around the crater rims, considered as a zone of the ejecta blanket. We remapped these blankets individually for the 20 largest impact basins (larger than 250 km) on Viking–MDIM–2 imagery. The image resolution (231 m/pxl) is sufficient to get a representative age, since most of the later geologic activity (mainly erosion) has the least effect in the large–crater size range (crater diameters larger than 3 km). Additional information for the interpretation of important geological units was obtained using Mars Orbiter Laser Altimeter topographic data. For these 20 basins with detectable ejecta blankets, the measured ages are within the expected range of 3.7 - 4.1 Ga (Tab. 13.1).

Name	Cen. Lat. & Lon.		Diameter km	Age Ga
Crater (smaller than 230 km)				
Gusev	14.7S	184.6W	166	4.02
Lowell	52.3S	81.4W	203	3.71
Crater (larger than 230 km)				
Flaugergues	17.0S	340.8W	245	–
Galle	51.2S	30.9W	230	–
Kepler	47.1S	219.1W	233	3.92
Lyot	50.8N	330.7W	236	3.40
Secchi	58.3S	258.1W	234	–
Crater (larger than 250 km)				
Antoniadi	21.5N	299.2W	394	3.79
Cassini	23.8N	328.2W	412	4.03
Copernicus	49.2S	169.2W	294	4.00
de Vaucouleurs	13.5S	189.1W	293	3.95
Herschel	14.9S	230.3W	304	3.95
Huygens	14.3S	304.6W	470	3.98
Koval'sky	30.2S	141.5W	309	3.96
Newcomb	24.4S	359.0W	252	4.00
Newton	40.8S	158.1W	298	4.11
Schiaparelli	2.7S	343.3W	471	3.92
Schroeter	1.9S	304.4W	292	3.92
Tikhonravov	13.5N	324.2W	386	4.10
Planitiae				
Argyre	50.0S	44.0W	800	3.83
Hellas	43.0S	290.0W	2200	3.99
Isidis	13.0N	273.0W	1200	3.96

Table 13.1.: List of the Martian impact basins. Location, diameter and resulting ages are given, see Fig. 13.2.

A few basins, where ejecta could not be identified due to obvious resurfacing processes, are suspected to be even older (possibly up to 4.2 Ga). The spacial distribution of Martian impact basins and their ages are summarized in Fig. 13.2. These basins are clearly situated in the heavily cratered highland unit (with an average age of about 4.0 Ga). Although some authors (e.g. Frey and Schultz, 1989) explain the formation of the northern lowlands as huge impact events (no clear evidence can be found) clearly distinguished basins are not found in the northern lowlands, with the exception of the relatively young and fresh-looking crater Lyot. It resembles a basin, but could also be classified simply as a large crater with a peak-ring. Our crater counts indicate an age of 3.4 Ga, while all other Martian basin ages average around 3.8 to 4.1 Ga.

Lunar Impact Basin Ages: In this study, lunar basin ages have been compiled bymaking use of the crater–frequency measurements obtained by Neukum (1983) and Wilhelms (1987). While 33 of the lunar basins were dated directly from cratering statistics, crater frequency measurements are non–existent for ten of the oldest basins of pre-Nectarian age (Wilhelms, 1987). In these cases, ages are determined by stratigraphic relationship to other basins. It is assumed that the South Pole-Aitkin basin age is roughly the same as the average lunar highland age (assumed to be 4.35 Ga). As a younger limit, Al-Khwarizmi/King is used, which has been dated in terms of superimposed crater frequency (Wilhelms, 1987) and is stratigraphically the youngest in the sequence of old basins (Tab. 13.2). The remaining basins are distributed between these two boundaries and slightly biased towards older ages (Tab. 13.2).

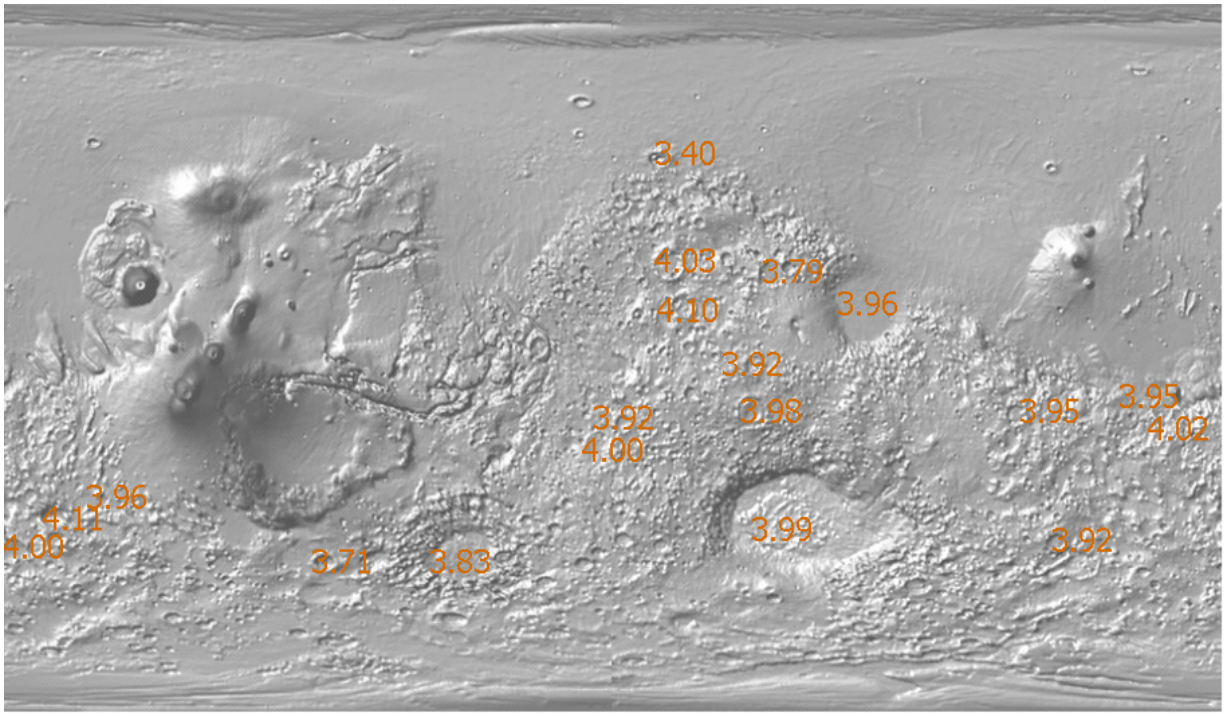

Figure 13.2.: The Martian basin ages are given here. The ages are superimposed on the location of the particular basin. The basemap is a shaded–relief based on MOLA data.

As previously discussed, the lunar basin ages range between 3.85 Ga and about 4.35 Ga, while the ages defined by crater counts range between 3.85 and 4.2 Ga. This upper limit is roughly for ages where saturation even in large crater diameter range still has no major affect.

Mars – Moon Comparison: The Martian surface we observe today appears to be no older than 4.2 Ga. As an important reference, Noachis Terra (the type region for the oldest stratigraphic sequence) shows an age of 4.02 Ga based on our crater counts and in accordance with the oldest basin ages. Almost all Martian basins are approximately 3.8 to 4.0 Ga old or younger, while datable lunar basins give ages between 3.85 and 4.3 Ga (Fig. 13.3). On average, lunar basins appear older, with the majority of occurrences prior to 4 Ga. The oldest surface units on the Moon are considered to be 4.35 Ga old (Wilhelms, 1987). The lunar distribution shows a maximum prior to 4 Ga ago, while the Martian data have a maximum basin

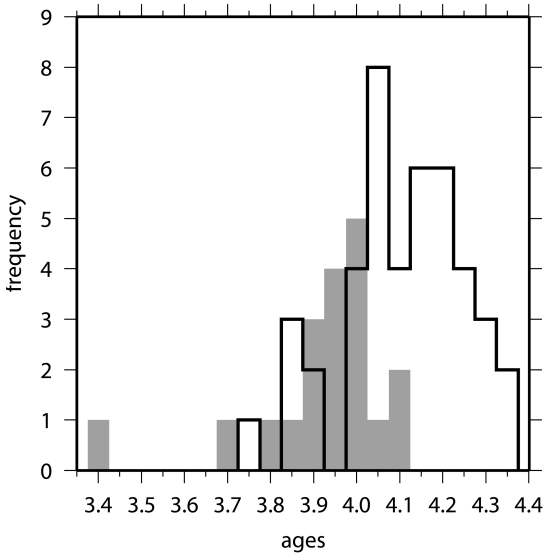

Figure 13.3.: The frequency distribution of the ages of lunar (open) and Martian (filled) impact basins given in this paper.

Name	Diameter km	Density $(10^6 km^2)^{-1}$	Age Ga
Pre–Nectarian Basins (stratigraphically related)			
Procellarum	3200		
South Pole–Aitken	2500		∼4.35
Tsiolkovskiy–Stark	700		
Grissom–White	600		
Insularum	600		
Marginis	580		
Flamsteed–Billy	570		
Balmer–Kapteyn	550		
Werner–Airy	500		
Pingré–Hausen	300		
Al-Khwarizmi/King	590	197	4.17
Pre–Nectarian Basins (ages based on crater frequencies)			
Fecunditatis	990		4.00
Australe	880	212	4.18
Tranquillitatis	800	A 11	3.73
Mutus-Vlacq	700	225	4.19
Nubium	690		4.00
Lomonosov-Fleming	620	177	4.15
Ingenii	650	162	4.14
Poincaré	340	190	4.16
Keeler-Heaviside	780	186	4.16⋆
Coulomb-Sarton	530	145	4.12
Smythii	840	166	4.14⋆
Lorentz	360	166	4.14⋆
Amundsen-Ganswindt	355	156	4.14
Schiller-Zucchius	325	112	4.09
Planck	325	110	4.08
Birkhoff	330	127	4.11⋆
Freundlich-Sharanov	600	129	4.11⋆
Grimaldi	430	97	4.06
Apollo	505	119	4.10⋆
Nectarian Basins (ages based on crater frequencies)			
Nectaris	860	79	4.03⋆
Mendel-Rydberg	630	73	4.02⋆
Moscoviense	445	87	4.05⋆
Korolev	440	79	4.03⋆
Mendeleev	330	63	4.00⋆
Humboldtianum	700	62	4.00⋆
Humorum	820	56	3.98⋆
Crisium	1060	53	3.97⋆
Serenitatis	740	83	4.04
Hertzsprung	570	58	4.04⋆
Sikorsky-Rittenhouse	310	27	3.87
Bailly	300	31	3.89

Table 13.2.: List of lunar impact basins. The crater frequencies are by Wilhelms (1987) and translated to ages, ages marked by ⋆ are ages from Neukum (1983).

occurrence at 4 Ga. This implies that the oldest Martian crustal structures observed today (based on crater counts) are no more than 4.2 Ga old, whereas the lunar surface record probably dates back to 4.3 or 4.4 Ga. On Mars, the earlier record has been erased by endogenic and surface erosional processes. The global basin record (diameters and location catalogued by Barlow (1988a)) supports these results, for discussion see Chap. 11.

In order to better compare the lunar and Martian basin population, we analyzed the frequency of basins with respect to the formation age plotted as a histogram (Fig. 13.3). The number of basins per age period is the same for both the Moon and Mars. Mars shows for the time span 3.7 - 4.0 Ga, a total of 16 basins, whereas the moon has 10 basins for the same age period. This is roughly in accordance with the fact that the Martian highland surface that contain basins is almost two times larger than the total surface of the Moon, which is the reference surface for the 43 basins studied here (Werner and Neukum, 2003).

13.2. Gusev Crater – The MER Spirit Landing Site

Among the previously discussed Martian impact basins, there is Gusev crater, the landing site of one of the two robot rovers of the American Mars Exploration Rover (MER) mission, which landed in January 2004. At the same time, the European Mars Express mission arrived at Mars. During its first year, Gusev Crater (about 160 km in diameter) has been imaged several times. The crater is situated at the dichotomy boundary (14.7°S and 175.3°E). directly south of the volcanic construct Apollinaris Patera. To the south, Ma'adim Vallis (valley), which cuts into highland terrain, incises the crater rim and widens into Gusev. The MER mission scientists hoped to find indications of a former lake within Gusev crater, which are allegedly sediments deposited by the Ma'adim Vallis (Squyres *et al.*, 2004b; Kuzmin *et al.*, 2000; Cabrol *et al.*, 2003). Other origins of the deposits that make up the crater floor have also been proposed (Greeley, 2003; Golombek *et al.*, 2003). Most of the Spirit MER lander instruments indicate that the rocks found on the Gusev floor are predominantly basaltic in composition. No evidence for rocks of primary sedimentary origin has been found, although the rocks are altered by weathering involving liquid water (McSween *et al.*, 2004; Gellert *et al.*, 2004; Christensen *et al.*, 2004; Morris *et al.*, 2004). Comparing Gusev crater (imaged by HRSC) and Grimaldi crater on the Moon (imaged by Lunar Orbiter), features inside Gusev crater clearly resemble "mare–type" wrinkle ridges. These are typical of deformation of basaltic lava flows (Greeley *et al.*, 2005), although landforms with a similar morphology can also be the result of compressional defomation of a sedimentray mantle (e.g. the Meckering fault in Australia; Gordon and Lewis, 1980). Based on morphologic data, Greeley *et al.* (2005) suggest that Gusev is flooded by lavas, a finding supported by the chemical and mineralogical findings of the MER lander instruments. The surrounding highland plateau of Gusev to the south and east is characterized by impact craters and inter–crater plains, while the area west of Gusev is dominated by low–lying plains of the impact basin de Vaucouleurs. Northeast of Gusev and east of Apollinaris Patera, the Medusae Fossae Formation is located, which is believed to be pyroclastic material and which is strongly wind–sculpted.

Using the HRSC, THEMIS and MOC imagery, the Gusev crater and its vicinity has been mapped by van Kan (2004). Her results are in approximate agreement with earlier morphological mapping attempts based on Viking imagery by Kuzmin *et al.* (2000) at an image resolution of about 70m/pxl and with a thermophysical characterization of Gusev's interior based mainly on thermal–infrared data from the thermal emission imaging system (THEMIS) at a resolution of 100m/pxl by Milam *et al.* (2003). Selected areas, with simplified unit boundaries representing the mapped units, were used to determine ages. These ages, based on crater frequencies measured on a mosaic of HRSC images obtained during orbits 24,72, 283, 335 with a mosaic resolution of 25 m/pxl, are used to reconstruct the geologic evolution of the Gusev region (Fig. 13.4).

Based on these ages, the following geologic history of the Gusev region can be ascertained: The plain surrounding Gusev, belonging to the heavily cratered highland unit, has a surface age older than 4.0 Ga. At around that time, Gusev itself was most likely formed (see impact basin ages listed in Chapter 13). Later, the plains unit as well as Gusev's interior experienced a resurfacing event, which filled both inter–crater depressions and Gusev, and ended at about 3.65 Ga ago. Subsequent resurfacing of the Gusev interior and its vicinity produced the wrinkled and etched units in the eastern part of Gusev at approximately 3.45 Ga ago. A similar geologic history was reported by Kuzmin *et al.* (2000), but they argued that the main depositional source should have been fluvial sedimentation from the precursor to Ma'adim Vallis and later Ma'adim Vallis itself. The volcanic activity associated

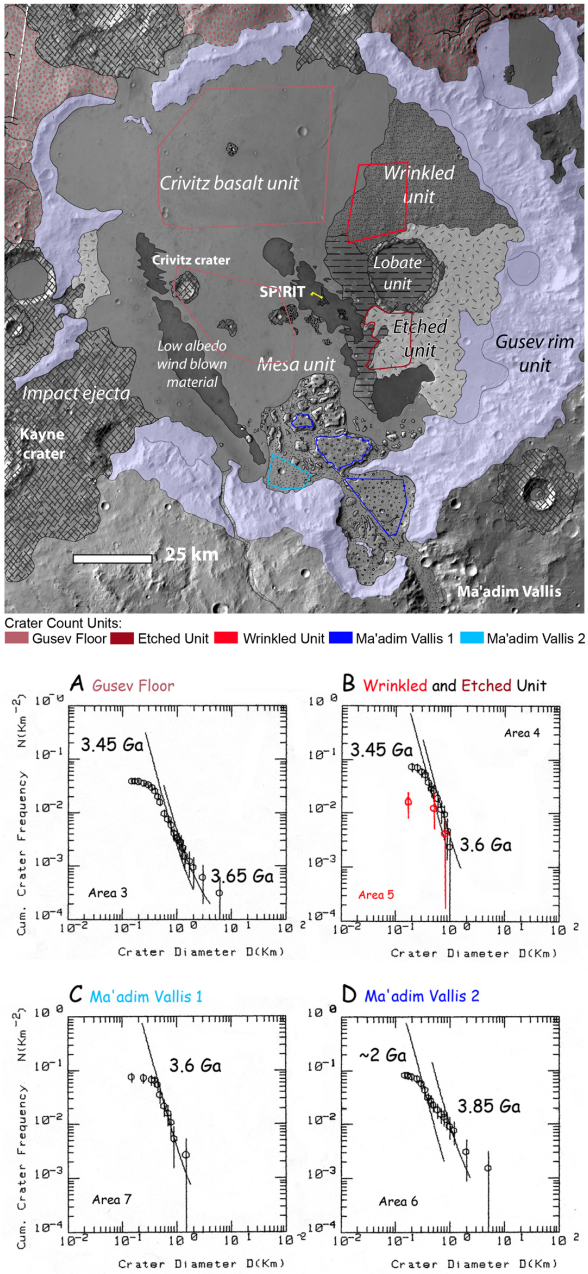

Figure 13.4.: A geologic map of the Gusev crater and its vicinity after van Kan (2004), and the outline of units used for crater counts and age determination. Below, the crater size-frequency distributions for the relevant units are given.

with Apollinaris Patera seems to be morphologically independent and ended already by about 3.75 Ga ago. While pyroclastic deposits of Apollinaris Patera could have contributed to the infill of Gusev, no clear stratigraphic and morphologic evidence is found. Possibly, the fluvial activity of Ma'adim Vallis started very early in Martian geologic history (about 3.85 Ga ago, Fig. 13.4 D) and appears to have ended about 2 Ga ago, at least resurfacing occurred further upstream Ma'adim Vallis. During this period, landforms, whose origin are possibly water related, formed elsewhere on the planet (see e.g. Chap. 14.4). Despite the geochemical evidence from volcanic material found at the Spirit traverse, fluvial deposits should have also contributed to Gusev's infill. Nevertheless, sediment discharge estimates from fluvial activity of Ma'adim Vallis could not solely fill Gusev's interior (Greeley *et al.*, 2005).

To better understand the contribution of volcanic or fluvial sediment infill into the initial impact depression, MOLA topographic profiles of similarly sized craters are investigated and compared with Gusev's morphometry. The size of the Gusev crater (diameter $\sim$ 160 km) suggests a complex internal structure, but the visible floor is very flat. Apparently, these selected craters, located in the Martian highlands, underwent a geological evolution different than Gusev. Nevertheless, most of the comparably sized craters appear partially filled, but some show a distinct central feature above the level of possible sedimentary infill. The two apparently least filled craters (43°S, 343°E and 23°S, 16°E) were used to estimate the Gusev infill (Fig. 13.5). Unlike Gusev, these two craters show a visible rim-to-floor depth of about 2.5 to 3 km, while for Gusev this is in the range of 1 to 1.5 km. Hence, the post–impact infilling of Gusev has a thickness of more than 1 to 1.5 km (Werner *et al.*, 2005a; Ivanov *et al.*, 2005). This is an important constraint for any assumed contribution from the earlier fluvial activity of Ma'adim Vallis and volcanic deposit thickness. The youngest formation in the vicinity of Gusev is the Medusae Fossae Formation ($\sim$ 1.6 Ga), which is a band along the dichotomy boundary between the two large volcanic provinces. Sim-

ilar ages are found in most locations (compare Chap. 14.4).

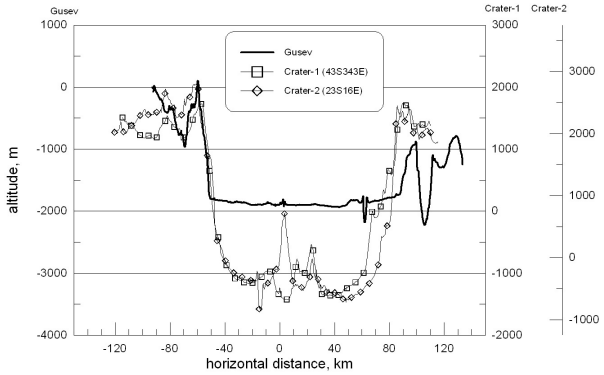

Figure 13.5.: Cross sections of Gusev and two craters of comparable size but less infill, indicating that the post–impact infilling of Gusev has a thickness of more than 1 to 1.5 km (Fig. from Ivanov *et al.* (2005) or Werner *et al.* (2005a)).

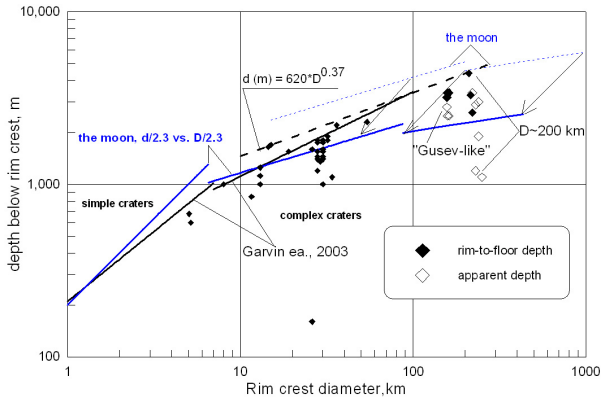

Figure 13.6.: Results of a simple approximate scaling of the depth-diameter relations from planet to planet to evaluate the depth–diameter relation of Gusev–sized craters (Fig. from Ivanov *et al.* (2005)).

Preliminary numerical modeling by Ivanov *et al.* (2005) indicates that the pristine cross section of Gusev–like craters on Mars shows a possible rim-to-floor depth of about 4 km. These model results are affected by the mechanical description of materials, including strength and dry friction for damaged rocks and the Acoustic Fluidization model, which simulates the assumed temporary dry friction reduction around the growing crater. To evaluate the model runs, results were compared with scaled depth/diameter relations for the Moon (Pike, 1977; Williams and Zuber, 1998). The assumption that the final crater shape is controlled by the balance between rock strength/friction and the lithostatic pressure allows us to propose a simple approximate scaling of the depth-diameter relations from planet to planet. In this approximated approach, complex craters with the same value of gD (g is the gravitational acceleration, D is crater diameter) should have a similarly scaled depth gd, where d is the crater depth (Fig. 13.6). The comparison of lunar depth–diameter relationships (Pike, 1977; Williams and Zuber, 1998) scaled to Mars gravity, Garvin et al.'s approximations (Garvin *et al.*, 2003), our previous measurements (Werner *et al.*, 2004a, see next Chapter) and new data for Gusev–like craters, support the maximum depth for a crater of 150 km in diameter and a final depth of the annular trough of about 4 km as stated in Ivanov *et al.* (2005)). Together with the measured results of craters of comparable size to Gusev, the model results constrain the relative thickness of fluvial and volcanic infill to approximately 1 to 1.5 km.